JACS
JOURNAL OF THE AMERICAN CHEMICAL SOCIETY

Communication

pubs.acs.org/JACS

Two-dimensional Covalent Organic Framework Thin Films Grown in Flow

Ryan P. Bisbey, Catherine R. DeBlase, Brian J. Smith, and William R. Dichtel*

Baker Laboratory, Department of Chemistry and Chemical Biology, Cornell University, Ithaca, New York 14853-1301, United States

Supporting Information

ABSTRACT: Two-dimensional covalent organic frameworks (2D COFs) are crystalline polymer networks whose modular 2D structures and permanent porosity motivate efforts to integrate them into sensing, energy storage, and optoelectronic devices. These applications require forming the material as a thin film instead of a microcrystalline powder, which has been achieved previously by including a substrate in the reaction mixture. This approach suffers from two key drawbacks: COF precipitates form concurrently and contaminate the film, and variable monomer and oligomer concentrations during the polymerization provide poor control over film thickness. Here we address these challenges by growing 2D COF thin films under continuous flow conditions. Initially homogeneous monomer solutions polymerize while pumped through heated tubing for a given residence time, after which they pass over a substrate. When the residence time and conditions are chosen judiciously, 2D COF powders form downstream of the substrate, and the chemical composition of the solution at the substrate remains constant. COF films grown in flow exhibit constant rates of mass deposition, enabling thickness control as well as access to thicker films than are available from previous static growth procedures. Notably, the crystallinity of COF films is observed only at longer residence times, suggesting that oligomeric and polymeric species play an important role in forming the 2D COF lattice. This approach, which we demonstrate for four different frameworks, is both a simple and powerful method to control the formation of COF thin films.

Covalent organic frameworks (COFs) are periodic two- or three-dimensional polymer networks whose topologies derive from the shape and functional group orientations of their monomers.[1] COFs have shown properties of interest for applications such as gas storage,[2] chemical separations,[3] catalysis,[4] and sensors,[5] as well as optoelectronic[6] and energy storage devices.[7] Many of these proposed uses will require growing COFs as thin films, ideally with control of their thickness, orientation, uniformity, and location. Layered 2D COF thin films have been obtained previously by submerging supported single-layer graphene,[8] Au,[7b] or indium tin oxide (ITO)[6b] substrates into the polymerization mixture. Although 2D COF films prepared in this manner exhibit preferential orientation of their crystallites and are amenable to further device fabrication steps, poor control over the polymerization remains a major limitation. Under these conditions, microcrystalline COF powders form concurrently, which contaminate the film.

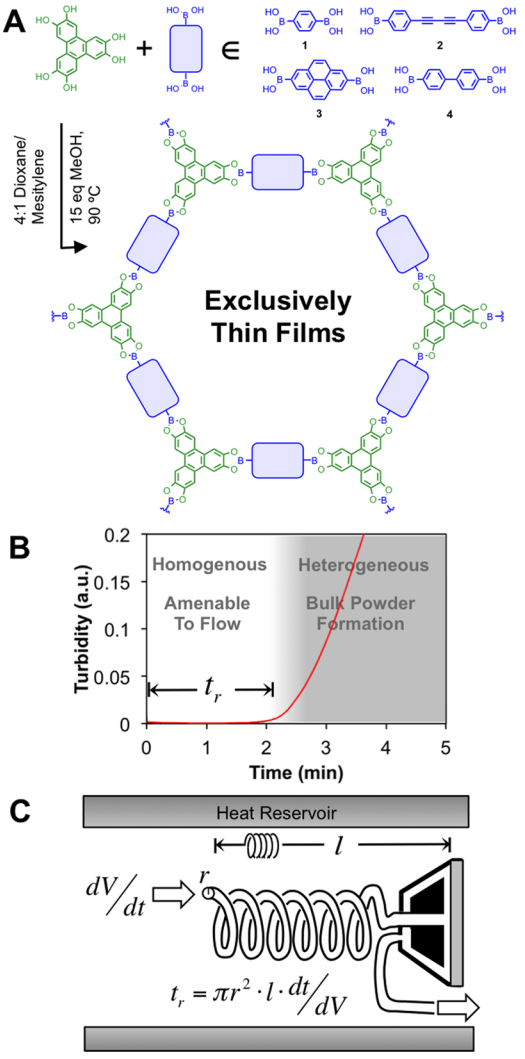

Figure 1. (A) General structure of 2D COFs formed from HHTP condensed with linear bis(boronic acid) **1**–**4**. (B) Turbidity as a function of reaction time during the formation of COF from homogeneous conditions provides an induction period amenable to a flow cell configuration. (C) Schematic of flow setup designed with variable induction period (see Figure S1 for photograph of the setup).

Received: May 5, 2016
Published: August 1, 2016

DOI: 10.1021/jacs.6b04669
J. Am. Chem. Soc. 2016, 138, 11433−11436

Furthermore, the concentrations of monomeric and oligomeric species vary during the polymerization, providing nonuniform film growth rates and poor thickness control. Adapting 2D COF thin film formation to a continuous flow process[9] overcomes these limitations because the chemical composition of the reactant solution at the substrate will be invariant, even over extended reaction times.

Here, we prepare 2D COF films using a flow cell, which provides unprecedented control of film thickness while avoiding contamination by bulk COF powders. These conditions provide access to arbitrarily thick films that grow at a constant rate. In contrast, the thicknesses of films grown under bulk conditions plateau at low maximum values and are difficult to control. Moreover, COF formation under these conditions is amenable for deriving additional mechanistic insight by varying the nature of the reactant solution and its polymerization time. Many solvothermal boronate ester-linked COF syntheses employ reaction conditions in which the monomers are only partially soluble, which are problematic for a flow cell configuration. We recently reported conditions to prepare boronate ester-linked 2D COFs that feature a homogeneous induction period prior to COF powder precipitation.[10] The induction period is reproducible and may be rationally manipulated by changing reaction parameters (e.g., concentration, temperature, presence of competitors). This reproducibility and flexibility are ideal for forming 2D COF thin films and probing their growth processes in flow.

The polymerization of HHTP and **1** to provide the boronate ester-linked framework, COF-5, was conducted in a flow cell using a dioxane/mesitylene solvent mixture with a small amount of MeOH added to dissolve both monomers (Figure 1). The monomers react slowly at 25 °C but condense to form COF-5 at 90 °C with an induction period of 2 min (Figure 1B). Growth in flow is achieved by pumping the reaction mixture through a reservoir heated to 90 °C and into a flow cell comprising a quartz crystal microbalance (QCM) substrate used to monitor mass deposition. The flow rate and/or tubing length may be varied to control the residence time (t_r), which is the period that the monomers are subjected to the polymerization conditions before reaching the substrate. When t_r is shorter than the induction period, the reaction solution remains homogeneous and does not clog the flow cell. Furthermore, t_r changes the reaction mixture's average degree of polymerization when it encounters the substrate: short t_r results in monomers and small oligomers reaching the substrate, whereas longer t_r results in larger species encountering the growth substrate. In contrast, a substrate submerged in a reaction mixture encounters solutions of variable concentration over the course of the reaction. Therefore, the flow cell configuration enables the rational study of reaction conditions for thin film formation, such as temperature, t_r, flow rate, and reaction mixture composition.

As evidence of this improved control of 2D COF thin film growth, COF-5 films prepared in flow deposit on the substrate at constant rates, as characterized by QCM. We initially selected a t_r of 60 s, which is half of the induction period observed in turbidity measurements. Under these conditions, a linear mass increase with respect to time is observed as approximated from the Sauerbrey eq (Figure 2A, black). The observed growth rate is 1.3 μg cm^{-2} min^{-1}, which is mirrored by a continuous increase in motional resistance of 0.46 kΩ s^{-1} (Figure 2B). The resistance change occurs because of viscoelastic losses, which is consistent with the deposition of a soft, porous film.[11] When such resistance increases are observed, the Sauerbrey mass generally over-

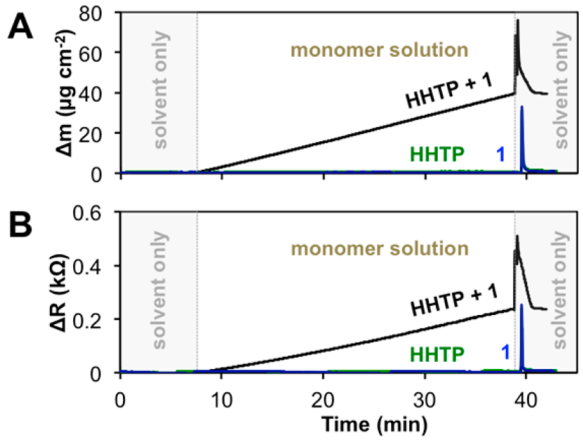

Figure 2. COF-5 thin film growth in flow as monitored by applying the Sauerbrey equation to the QCM frequency response (A) and resistance (B). A constant rate of polymer formation on the substrate is observed when both monomers are present (black traces). No changes in frequency or resistance are observed when solutions containing only HHTP (green traces) or **1** (blue traces) are used.

estimates the actual gravimetric mass deposited. This is the case for the COF-5 films, and we generated a calibration curve to correlate the film thickness, as measured by AFM, with the Sauerbrey mass (Figure S3). After 40 μg cm^{-2} was deposited, the reactant solution was replaced with the pure reaction solvent, after which film deposition stopped. Furthermore, the presence of both monomers is necessary for film growth, as no mass deposition or resistance change is observed when solutions containing only HHTP or **1** are used (Figure 2, green and blue traces). The rate of COF film formation remains constant throughout the polymerization process. Provided that t_r is shorter than the induction period, the COF does not precipitate in the flow cell or tubing, allowing films to be deposited at a constant rate for indefinite periods.

We also measured the rate of film deposition under a variety of conditions by reducing the monomer concentration or temperature, as well as by introducing inhibitors MeOH and H_2O (Figure S4). As expected, each of these changes result in slower growth rates, providing many independent experimental parameters. For a given set of growth conditions, the mass deposition is relatively consistent, as demonstrated for three independent experiments whose growth rates were within 15% of each other (Figure S5). We also examined the effect of varying the flow rate at a constant t_r, which did not affect the rate of film deposition strongly, suggesting that shear forces from the flowing solution do not influence COF film formation (Figure S6). These combined observations demonstrate a versatile and reliable method to grow COF films with superior control over thickness and rate relative to established bulk methods.

Growing COF thin films in flow provides a powerful opportunity to study the poorly understood polymerization and crystallization processes of these macromolecular architectures. The flow cell configuration exposes the growth substrate to specific and invariant mixture of monomers and condensed species, whose composition may be controlled by varying t_r, monomer concentration, temperature, and other reaction parameters. Most notably, by varying t_r, we found that the growth rate and crystallinity as assessed by *ex situ* grazing incidence X-ray diffraction (GI-XRD) of COF-5 films grown to the same Sauerbrey mass (10 μg cm^{-2}, Figure 3) vary dramatically. Crystalline, oriented thin films were formed only

DOI: 10.1021/jacs.6b04669
J. Am. Chem. Soc. 2016, 138, 11433−11436

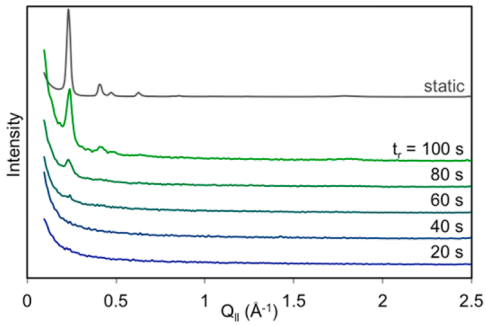

Figure 3. Integrated intensities ($Q_\perp$ = [0.3, 0.6] vs $Q_{||}$) of GI-XRD patterns of films grown to the same mass (10 μg cm^{-2}) at different t_r. GI-XRD of a film grown under static conditions; grown from identical conditions is included for reference.

at the longest values of t_r (80 and 100 s), whereas films grown using a short t_r (20 and 40 s) appear amorphous. These crystalline films are oriented parallel to the substrate (Figure S8), similar to COF films grown under bulk conditions.[8] The rate of film deposition also depends strongly on t_r, as growth rates increase 4-fold over the t_r range 10−50 s (Figure S7). Films formed at short t_r grow slowly and do not diffract X-rays in a manner consistent with COF-5. Reaction mixtures subjected to a longer t_r contain higher molecular weight species, which deposit on the substrate at a faster rate and provide crystalline COF-5 films. The relative degree of crystallinity, as judged by the intensity of the diffraction peaks of films grown to identical mass density, increases with t_r. Finally, subjecting amorphous films to a flow of dry solvent without monomers at 90 °C for 3 h did not anneal the film to the crystalline structure. These latter observations suggest that films are kinetically trapped in the phase in which they were deposited.

The growth of 2D COF films in flow is general with respect to other boronate ester-linked networks. A series of 2D hexagonal COFs, DPB-COF, TP-COF, and COF-10, which are derived from the condensation of HHTP with bis(boronic acid) linkers **2**, **3**, and **4**, respectively, were grown in flow. For each COF, t_r was selected as 90% of the induction period observed for its growth in solution. Under these conditions, each COF polymerization provides nearly constant rates of film deposition (Figure 4, blue traces). In contrast, films grown under static conditions exhibited growth profiles with an initial deposition whose rates varied unpredictably, after which the growth rate slowed and the total deposited mass per unit substrate area plateaued. COF-10 shows a slight slowing of the growth rate over 60 min, which we attribute to a decrease of the flow rate associated with partial clogging of the QCM flow cell outlet over long growth times. The thickness of COF films was further characterized using profilometry, which confirmed that the films grown in flow were thicker than those grown under static conditions (Table S1). Each film was further characterized by grazing incidence FT-IR spectroscopy, AFM, and SEM. The IR spectra of each 2D COF film was similar, independent of whether it was grown in flow or under static conditions (Figure S10) and correlated well to spectra of the bulk microcrystalline powder. These observations indicate that similar networks without major contamination from the monomers are formed in all cases. AFM and SEM of each film indicate that films grown in flow are less rough and contaminated by fewer particulates (Figures S11−S18) over large areas. These observations indicate that the growth of COF films in flow enables control of film thickness as well as access to thicker films than are formed under bulk growth conditions. Films grown in flow are more smooth and less contaminated by particulates on their top surfaces.

The flow cell configuration also enables the characterization of the stability of COF films to water and other compounds that induce dissolution. To evaluate this possibility, we flowed 4:1 dioxane/mesitylene solutions at 1 mL min^{-1} containing 120 mM H_2O, MeOH, 4-*tert*-butylphenylboronic acid, or 4-*tert*-butylcatechol over crystalline COF-5 films grown to the same mass (10 μg cm^{-2}). All four species have been studied as additives during COF growth, and water has been studied for the dissolution.[10a,12] The concentration of these additives corresponds to ∼2000-fold excess of the etchant species per milliliter of solution. As expected, the COF-5 films lose mass when exposed to wet solvent (Figure 5, blue), corresponding to the hydrolysis of their boronate ester linkages. Dissolution of the films is also observed in the presence of MeOH (Figure 5, red). In contrast, neither the catechol nor phenylboronic acid species caused the films to lose significant mass, with the minor decrease observed at the beginning of the process (Figure 5, green and purple, respectively) consistent with that observed when newly grown films are subjected to a flow of the pure solvent mixture. This observation indicates that the boronic esters of the COF-5 films are not in dynamic equilibrium with catechol or boronic acid species in solution.

In conclusion, we have formed the first 2D COF thin films using a flow cell configuration, which has numerous advantages relative to including a substrate in the bulk polymerization. This method is the first general strategy to control film thickness, as films are deposited at a nearly constant rate. In contrast, the continuous formation of COF powders under bulk conditions causes the solution composition of monomers and oligomers to change dramatically over the course of film growth. Using a QCM flow cell for the film growth provides the level of sensitivity necessary to gain insight into the COF film growth mechanism. We observe both faster growth and crystallinity only at long induction periods, indicating that crystalline films are likely

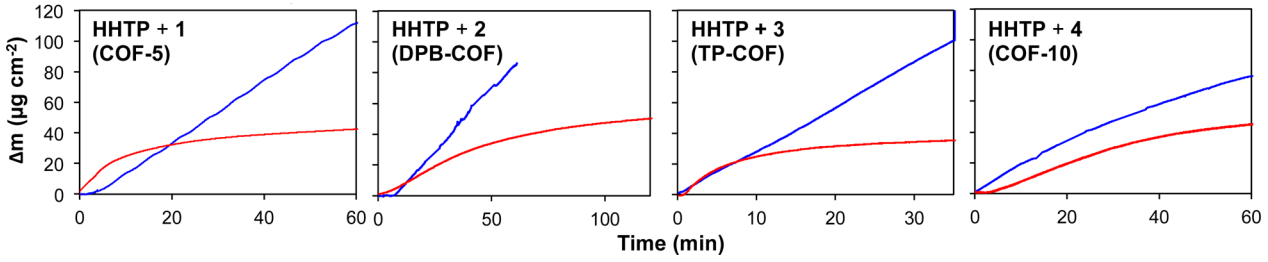

Figure 4. COF film growth in flow (blue traces) versus static (red traces) for various boronic acids condensed with HHTP: COF-5, DPB-COF, TP-COF, and COF-10 (from left to right).

DOI: 10.1021/jacs.6b04669
J. Am. Chem. Soc. 2016, 138, 11433−11436

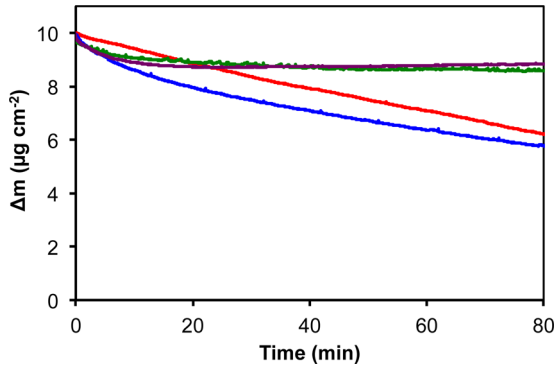

Figure 5. COF-5 films grown to approximately 10 μg cm^{-2} subjected to 0.5 mL min^{-1} flow of 120 mM of various species in 4:1 dioxane/mesitylene. Film dissolution is observed for H_2O and MeOH (blue and red traces, respectively) but not *t*-butyl catechol nor *t*-butylphenyl boronic acid (green and purple traces, respectively).

derived from the addition of larger oligomeric species to the substrate, not monomers.[13] The films are found to etch with exposure to H_2O and MeOH but not catechol and boronic acid species, indicating that amorphous film may be kinetically trapped from processes such as error correction and crystallization. Given the importance of the thin film morphology for integrating emerging COF materials into optoelectronic and energy storage devices, these findings will enable new methods for oriented COF thin films to be synthesized affording control over thickness while preventing contamination of the film by bulk powder precipitates.

■ ASSOCIATED CONTENT

Supporting Information

The Supporting Information is available free of charge on the ACS Publications website at DOI: 10.1021/jacs.6b04669.

Experimental procedures, additional QCM data, 2D GI-XRD patterns, profilometry data, AFM micrographs, SEM images, and FT-IR spectra (PDF)

■ AUTHOR INFORMATION

Corresponding Author

*wdichtel@cornell.edu

Notes

The authors declare no competing financial interest.

■ ACKNOWLEDGMENTS

R.P.B. acknowledges support from the NSF IGERT program (DGE-0903653). W.R.D. acknowledges the Army Research Office for a Multidisciplinary University Research Initiatives (MURI) award under grant number W911NF-15-1-0447. This work is based upon research conducted at the Cornell High Energy Synchrotron Source (CHESS), which is supported by the NSF and the NIH/NIGMS (DMR-1332208). This research made use of facilities supported by the NSF (DMR-1120296).

■ REFERENCES

(1) (a) Ding, S.-Y.; Wang, W. *Chem. Soc. Rev.* **2013**, *42*, 548−568. (b) Feng, X.; Ding, X.; Jiang, D. *Chem. Soc. Rev.* **2012**, *41*, 6010−6022. (c) Colson, J. W.; Dichtel, W. R. *Nat. Chem.* **2013**, *5*, 453−465. (d) Jackson, K. T.; Reich, T. E.; El-Kaderi, H. M. *Chem. Commun.* **2012**, *48*, 8823−8825. (e) Tilford, R. W.; Mugavero, S. J., III; Pellechia, P. J.; Lavigne, J. J. *Adv. Mater.* **2008**, *20*, 2741−2746. (f) DeBlase, C. R.; Dichtel, W. R. *Macromolecules* **2016**, DOI: 10.1021/acs.macromol.6b00891.

(2) (a) Rabbani, M. G.; Sekizkardes, A. K.; Kahveci, Z.; Reich, T. E.; Ding, R.; El-Kaderi, H. M. *Chem. − Eur. J.* **2013**, *19*, 3324−3328. (b) Doonan, C. J.; Tranchemontagne, D. J.; Glover, T. G.; Hunt, J. R.; Yaghi, O. M. *Nat. Chem.* **2010**, *2*, 235−238.

(3) (a) Yang, C.; Liu, C.; Caoa, Y.; Yan, X. *Chem. Commun.* **2015**, *51*, 12254−12257. (b) Oh, H.; Kalidindi, S. B.; Um, Y.; Bureekaew, S.; Schmid, R.; Fischer, R. A.; Hirscher, M. *Angew. Chem., Int. Ed.* **2013**, *52*, 13219−13222. (c) Keskin, S. *J. Phys. Chem. C* **2012**, *116*, 1772−1779.

(4) (a) Xu, H.; Gao, J.; Jiang, D. *Nat. Chem.* **2015**, *7*, 905−912. (b) Lin, S.; Diercks, C. S.; Zhang, Y.; Kornienko, N.; Nichols, E. M.; Zhao, Y.; Paris, A. R.; Kim, D.; Yang, P.; Yaghi, O. M.; Chang, C. J. *Science* **2015**, *349*, 1208−1213. (c) Xu, H.; Chen, X.; Gao, J.; Lin, J.; Addicoat, M.; Irle, S.; Jiang, D. *Chem. Commun.* **2014**, *50*, 1292−1294. (d) Fang, Q.; Gu, S.; Zheng, J.; Zhuang, Z.; Qiu, S.; Yan, Y. *Angew. Chem., Int. Ed.* **2014**, *53*, 2878−2882. (e) Shinde, D. B.; Kandambeth, S.; Pachfule, P.; Kumar, R. R.; Banerjee, R. *Chem. Commun.* **2015**, *51*, 310−313. (f) Ding, S.-Y.; Gao, J.; Wang, Q.; Zhang, Y.; Song, W.-G.; Su, C.-Y.; Wang, W. *J. Am. Chem. Soc.* **2011**, *133*, 19816−19822.

(5) (a) Das, G.; Biswal, B. P.; Kandambeth, S.; Venkatesh, V.; Kaur, G.; Addicoat, M.; Heine, T.; Verma, S.; Banerjee, R. *Chem. Sci.* **2015**, *6*, 3931−3939. (b) Dalapati, S.; Jin, S.; Gao, J.; Xu, Y.; Nagai, A.; Jiang, D. *J. Am. Chem. Soc.* **2013**, *135*, 17310−17313.

(6) (a) Guo, J.; Xu, Y.; Jin, S.; Chen, L.; Kaji, T.; Honsho, Y.; Addicoat, M. A.; Kim, J.; Saeki, A.; Ihee, H.; Seki, S.; Irle, S.; Hiramoto, M.; Gao, J.; Jiang, D. *Nat. Commun.* **2013**, *4*, 2736. (b) Dogru, M.; Handloser, M.; Auras, F.; Kunz, T.; Medina, D.; Hartschuh, A.; Knochel, P.; Bein, T. *Angew. Chem., Int. Ed.* **2013**, *52*, 2920−2924.

(7) (a) DeBlase, C. R.; Silberstein, K. E.; Truong, T.; Abruña, H. D.; Dichtel, W. R. *J. Am. Chem. Soc.* **2013**, *135*, 16821−16824. (b) DeBlase, C. R.; Hernández-Burgos, K.; Silberstein, K. E.; Rodríguez-Calero, G. G.; Bisbey, R. P.; Abruña, H. D.; Dichtel, W. R. *ACS Nano* **2015**, *9*, 3178−3183. (c) Chandra, S.; Kundu, T.; Kandambeth, S.; BabaRao, R.; Marathe, Y.; Kunjir, S. M.; Banerjee, R. *J. Am. Chem. Soc.* **2014**, *136*, 6570−6573.

(8) (a) Colson, J. W.; Woll, A. R.; Mukherjee, A.; Levendorf, M. P.; Spitler, E. L.; Shields, V. B.; Spencer, M. G.; Park, J.; Dichtel, W. R. *Science* **2011**, *332*, 228−231. (b) Colson, J. W.; Mann, J. A.; DeBlase, C. R.; Dichtel, W. R. *J. Polym. Sci., Part A: Polym. Chem.* **2015**, *53*, 378−384.

(9) (a) Adamo, A.; Beingessner, R. L.; Behnam, M.; Chen, J.; Jamison, T. F.; Jensen, K. F.; Monbaliu, J.-C. M.; Myerson, A. S.; Revalor, E. M.; Snead, D. R.; Stelzer, T.; Weeranoppanant, N.; Wong, S. Y.; Zhang, P. *Science* **2016**, *352*, 61−67. (b) Leibfarth, F. A.; Johnson, J. A.; Jamison, T. F. *Proc. Natl. Acad. Sci. U. S. A.* **2015**, *112*, 10617−10622. (c) Peng, Y.; Wong, W. K.; Hu, Z.; Cheng, Y.; Yuan, D.; Khan, S. A.; Zhao, D. *Chem. Mater.* **2016**, *28*, 5095. (d) Rodríguez-San-Miguel, D.; Abrishamkar, A.; Navarro, J. A. R.; Rodriguez-Trujillo, R.; Amabilino, D. B.; Mas-Ballesté, R.; Zamora, F.; Puigmartí-Luis, J. *Chem. Commun.* **2016**, *52*, 9212−9215.

(10) (a) Smith, B. J.; Dichtel, W. R. *J. Am. Chem. Soc.* **2014**, *136*, 8783−8789. (b) Smith, B. J.; Hwang, N.; Chavez, A. D.; Novotney, J. L.; Dichtel, W. R. *Chem. Commun.* **2015**, *51*, 7532−7535.

(11) In this case the Sauerbrey mass is not a direct measure of the deposited mass. Viscoelastic losses between the porous film and solvent contribute to the frequency decrease, such that the Sauerbey mass overestimates the deposited mass. However, the Sauerbrey mass remains proportional to the gravimetric mass as long as the resistance change is constant.

(12) (a) Calik, M.; Sick, T.; Dogru, M.; Döblinger, M.; Datz, S.; Budde, H.; Hartschuh, A.; Auras, F.; Bein, T. *J. Am. Chem. Soc.* **2016**, *138*, 1234−1239. (b) Lanni, L. M.; Tilford, R. W.; Bharathy, M.; Lavigne, J. J. *J. Am. Chem. Soc.* **2011**, *133*, 13975−13983.

(13) Lupulescu, A. I.; Rimer, J. D. *Science* **2014**, *344*, 729−732.